

# A NONLINEAR, INERTIAL-TYPE APPROXIMATION OF THE PNEUMATIC ARTIFICIAL MUSCLE MODEL. EXPERIMENTAL DETERMINATION OF THE EQUIVALENT FREQUENCY TRANSFER FUNCTION

Adrian DĂNILĂ, Ioana Mădălina PETRE

Transilvania University of Brasov, Romania

**Abstract.** At present the pneumatic artificial muscle is largely used in powerful robot-arms and machine-to-human interfaces. This paper focuses on the modelling of the pneumatic artificial muscle. The first theoretical part of the paper, presents the main models of the pneumatic artificial muscle discussed in literature. The second theoretical part of the paper addresses the equivalence between the non-inertial hysteresis model of the muscle and an inertial equivalent elliptical hysteresis model. In the experimental part of the paper, the experimental setup and the computational methods are presented. The numerical results and the conclusions are presented in the final part of the paper.

**Keywords:** hysteresis, modelling, nonlinear systems, pneumatic artificial muscle

## 1. Introduction

The pneumatic artificial muscle (PAM) invented in the 1950s has been largely analysed in recent years, as Japanese engineers from Bridgestone redesigned and implemented PAM into powerful robot arms.

The PAM is used to convert pneumatic power into mechanical displacement. When inflated, the PAM is enlarged in radial direction and shortened in longitudinally. The contracting force of the muscle is unidirectional and features a non-linear dependence versus the inlet pressure. The PAM highly complies with the human muscle; therefore it is also suitable for human recovery apparatus, Figure 1.



Figure 1. A human recovery apparatus motorized with a pneumatic artificial muscle of type MAS-20-750N-AAMC-O-ER-BG (Festo AG & CO)

Besides these advantages, the PAM exhibits two main drawbacks that limit its applications: (1) the nonlinearity of the pressure build-up and (2) the hysteresis due to the structure geometry and to the operation principle [1].

The robot-arm implementations of PAM require accurate slider-mode control systems that compensate the drawbacks mentioned above [4].

Within this approach several papers in literature, such as [1, 2, 7], extensively address modelling of PAM. The majority of the models presented in literature are empirical process analysis models.

In this paper the authors propose a new approach to PAM modelling based on the equivalence of the non-inertial hysteresis to an inertial elliptical hysteresis. This approach is similar to the linearization of the model of an electromagnetic actuator with iron core losses.

The main advantage of the proposed approach is that the resulting model parameters can be obtained directly from the recorded data, allowing determination of the control law.

## 2. Overview of PAM modelling

### 2.1. Static Modelling of the PAM

Static modelling of PAM by means of empirical process analysis is presented in [1, 2]. Empirical models are developed from experiments performed in controlled and imposed conditions and based on simplification hypotheses. A static force generator model is presented in [2], based on isometric contraction, *i.e.* at constant length of the PAM. The experimental results validate the following properties of the PAM materialised in the considered force generator model: (1) The static force is globally proportional to the cross-sectional area  $S$  of the muscle, (2) the static force is globally independent of the initial length of the muscle, (3) the static force is globally proportional to the control pressure  $p$  (4) the maximum static force increases as the initial braid angle of the muscle decreases, (5) the static force decreases almost linearly with the contraction ratio  $\varepsilon = \Delta l/l_0$  according to a slope globally proportional to the control pressure  $p$ .

The expression of the PAM force given in [2] is:

$$F(\varepsilon, p) = S \cdot p \cdot \left[ a \cdot (1 - k \cdot \varepsilon)^2 - b \right], \quad (1)$$

where  $a = 3 \cdot \tan^2(\alpha_0)$  and  $b = 1/\sin^2(\alpha_0)$  are geometrical parameters depending on the initial angle of the braided shell  $\alpha_0$  and  $k \in (0; 1)$  is a coefficient that takes into account the decrease of the active cylindrical part due to the increase of the tapered shape at both ends when the PAM contracts. Similar expressions for the static force were reported in [5] and [7].

In this paper the static force is derived from the continuous component resulting from frequency analysis.

### 2.2. Stationary Modelling of the Presliding Regime of the PAM

If tested under isobaric and isotonic conditions, the PAM behaves nonlinearly with hysteresis non-local memory, Figure 2.

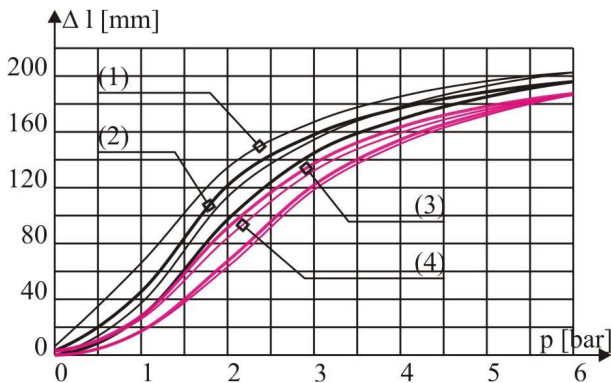
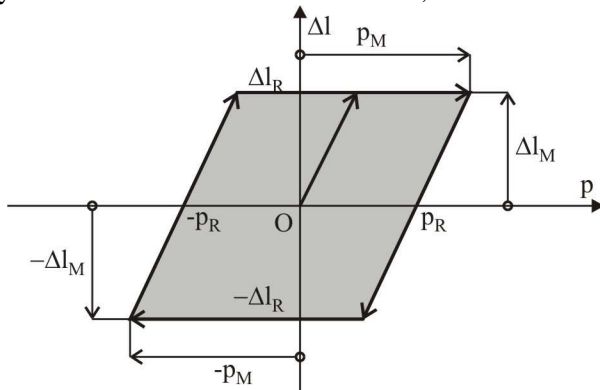


Figure 2. Experimental determinations of the PAM hysteresis. Device type: MAS-20-750N-AAMC-O-ER-BG; amplitude of the input pressure: (1)  $p = 1$  bar, (2)  $p = 3$  bar, and (3)  $p = 5$  bar

This behaviour is caused by the inherent hysteresis of the elastic bladder, the friction



between the braided cords and the rubber bladder, and the friction between the cords themselves.

As reported in the literature the most significant contribution to this phenomenon is caused by the dry friction between the cords [1].

A study of the dry friction between two surfaces, made by Swevers et al. emphasised two distinct regimes of the phenomenon: (a) the presliding regime where the asperity junctions deform elasto-plastically resulting in non-linear spring behaviour and (b) the sliding regime that occurs when the displacement increases until the asperity contacts are broken away.

The friction force  $F(x)$  for a contraction  $x$  can be expressed by the state equation below [1]

$$F(x) = F_M + 2 \cdot F_v \left( \frac{x - x_M}{2} \right), \quad (2)$$

where  $F_M$  is the friction force at the reversal point  $x_M$  of the hysteresis curve and

$$F_v(\xi) = \begin{cases} F_{ini}(\xi) & ; \xi \geq 0 \\ -F_{ini}(-\xi) & ; \xi < 0 \end{cases} \quad (3)$$

$F_{ini}$  is the virgin curve.

### 2.3. The Maxwell-Slip Model of the PAM Hysteresis

The Maxwell-slip model can be obtained by piecewise-linearization approximation of the virgin curve, characterizing the friction during presliding [1], Figure 3.

A more accurate model was developed by Iwan, where several contributing elements as shown in Figure 2 are referred to as Maxwell-slip model contributing elements. All the contributing elements are parallel connected such as to model the complex behaviour of nonlocal memory hysteresis at any instant [1].

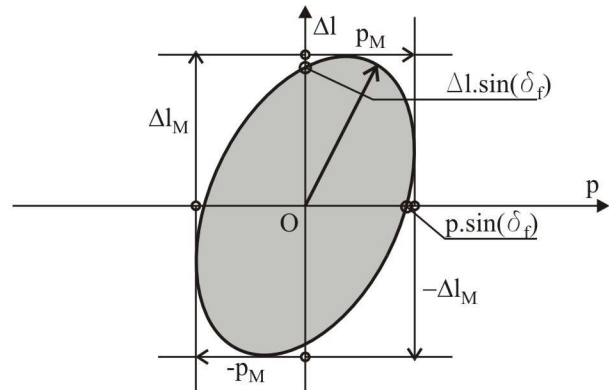


Figure 3. Modelling hysteresis using the Maxwell-slip model - to the left, and non-inertial elliptical hysteresis model - to the right

The virgin curve can be experimentally obtained by exciting the muscle to its maximum length. Then the number of representing Maxwell-slip elements and their characteristics can be intuitively selected from the given virgin curve. From the theoretical point of view, the PAM contraction is a non-inertial hysteresis process with memory.

Several other technical processes feature the same behaviour such as the electromagnetic actuator with iron losses. The static linearization of the hysteresis of the electromagnetic actuator with iron losses, presented in literature [3] is based on the equivalence of the non-inertial hysteresis and the elliptical inertial hysteresis. In the following the authors of this paper implemented this approach for the PAM hysteresis modelling.

### 3. The Equivalence of the PAM Hysteresis to an Elliptical Inertial Hysteresis

#### 3.1. The Model of the Electromagnetic Actuator with Core Iron Losses

The analysis and design of the Electromagnetic Actuator with Core Iron Losses is based on the equivalent sine current [3]. In this approach, the non-inertial hysteresis model of the actuator is equivalent to the inertial elliptical hysteresis. The equivalence between the two models is given by the equality of the power losses, Figure 3.

In this approach, the equivalent inertial elliptical hysteresis model will be given by the following expression:

$$\frac{p^2(t)}{p_M^2} + \frac{\Delta l^2(t)}{\Delta l_M^2} - 2 \cdot \frac{p(t) \cdot \Delta l(t)}{p_M \cdot \Delta l_M} \cdot \cos(\delta_f) = \sin^2(\delta_f) \quad (4)$$

where  $p(t)$ ;  $\Delta l(t)$  are the time dependencies of variable components of the inlet pressure and the PAM compression, respectively,  $p_M$ ;  $\Delta l_M$  are the amplitudes of the variable components of the inlet pressure and PAM compression, and  $\delta_f$  is the equivalent loss angle.

### 4. The Experimental Implementations and Results

The basic setup of the experiment used a PAM of type MAS-20-750N-AA-MC-O-ER-BG (Festo AG & CO) on the rehabilitation equipment shown in Figure 1 [8, 9].

The input pressure was controlled, measured and recorded revealing a sinusoidal time dependency. The amplitude and the frequency of the pressure vs. time dependency were prescribed.

The contraction of the PAM studied in the experiment was measured and recorded. The equipment used for the experiment consisted of (1) an analogue pressure transducer (input 0 ÷ 10 bar, output 0 ÷ 10 V), (2) an analogue displacement transducer and (3) a data acquisition board of type EasyPort for the acquired data conditioning. The associated software environment, FluidLab®-P V1.0, allowed the graphical representation of both acquired and estimated data.

Figure 2 shows the PAM hysteresis for several input pressures.

The time dependency of the input pressure and output contraction are given in Figure 4.

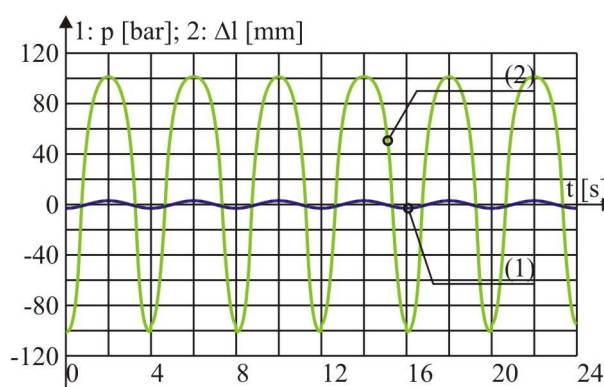


Figure 4. The time dependency of the PAM contraction - curve (2), for a sinusoidal dependency of the inlet pressure - curve (1);  $p(t) = 3 \cdot \sin(\omega_1 \cdot t - \pi/2)$  [bar];  $\omega_1 = \pi/2$  [rad/s] and  $f_1 = 0.25$  Hz

The proposed method uses the Fourier analysis to determine the continuous component and the harmonics of the PAM contraction versus time dependency.

For this purpose the acquired data was used as input data of a software application written in SCILAB software environment.

The harmonic components of the contraction dependency are given in Table 1, Table 2 and in Figures 5 and 6.

Table 1. The amplitude of the harmonic components of the PAM contraction vs. time dependency; input pressure  $p = 6$  bar

Denomination	Amplitude	Frequency
Continuous component	126.91939	0.0417
First Harmonic	2.75486	0.1667
Second Harmonic	51.06844	0.2917
Third Harmonic	4.04428	0.4167
Fourth Harmonic	14.71742	0.5417
Fifth Harmonic	1.61841	0.6667
Sixth Harmonic	2.97579	1.0417

Table 2. The Phase Angle of the Harmonic Components of the PAM Contraction vs. Time Dependency; input pressure  $p = 6$  bar

Denomination	Amplitude	Frequency
Continuous component	0.0	0.0417
First Harmonic	-1.5651	0.1667
Second Harmonic	0.0	0.2917
Third Harmonic	-1.5669	0.4167
Fourth Harmonic	0	0.5417
Fifth Harmonic	-1.5611	0.6667
Sixth Harmonic	0	1.0417

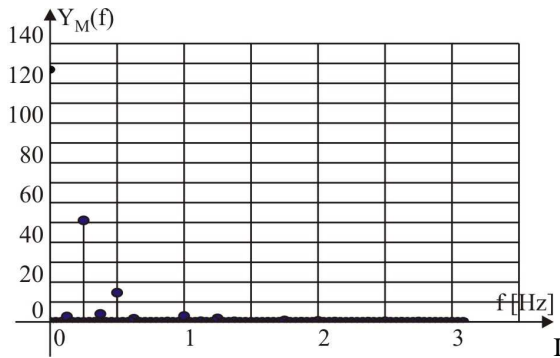


Figure 5. The amplitude spectra of the PAM contraction

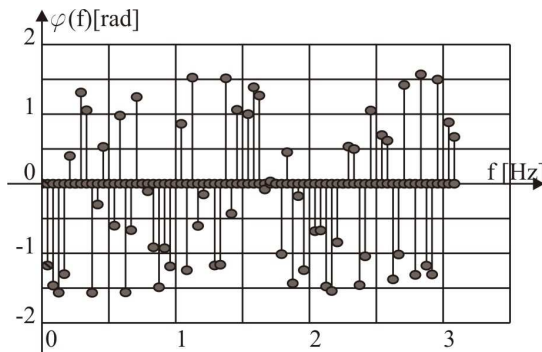


Figure 6. The phase-angle spectra of the PAM contraction

Further on only the variable components will be considered. In this case, the response  $y(t)$  of the linear - time, invariant system to a sinusoidal input  $u(t) = U_M \sin(\omega t)$  is given by the following expression [6]:

$$y(t) = Y_M \cdot \sin(\omega \cdot t + \arg\{G(j \cdot \omega)\}) \quad (5)$$

$$Y_M = U_M \cdot |G(j \cdot \omega)|$$

where  $G(j \cdot \omega) = |G(j \cdot \omega)| \cdot e^{j \cdot \arg\{G(j \cdot \omega)\}}$  is the transfer function of the system.

Based on the results above and taking into account the second harmonic only, in the hypothesis that the PAM behaves like a first order element the expression below has been determined for the equivalent transfer function:

$$G(j \cdot \omega) = \frac{k_a}{1 + j \cdot T_f \cdot \omega} = \frac{9.3}{1 + j \cdot 14.9 \cdot \omega} \quad (6)$$

By means of the resulting frequency transfer-function, the equivalent transfer function results immediately.

Figure 7 presents a comparison between the per-unit input pressure and the average estimation of the contraction response computed by means of the equivalent transfer function.

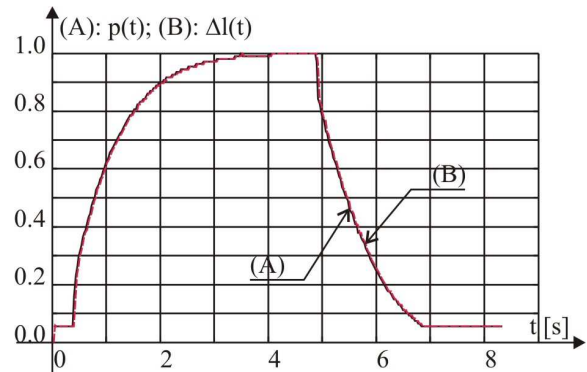


Figure 7. The per-unit input pressure, from the experimental data - curve (A) and the per-unit contraction of PAM - curve (B) estimated by means of the linearized transfer function

Based on these results the delay between the command pressure and the response of the PAM was computed. The resulting estimated delay is of 0.3 s.

## 5. Conclusions

In this paper the authors emphasized a possible similarity between the PAM model and the linearized model of the electromagnetic actuator with core iron losses.

Based on the losses equivalence, the non-inertial hysteresis of the PAM may be equivalent to an elliptical inertial hysteresis model. This approach allows the development of an equivalent linear model of the PAM. Under the assumption that the equivalent model of the PAM has the form of a first-order element, only two parameters have to be determined. The estimation of these parameters is straightforward if the amplitude and the phase angle of the harmonics are available from data.

The proposed approach is particularly useful for the dynamic control of the PAM.

## Acknowledgment

This paper is supported by the Sectoral Operational Program Human Resources Development (SOP HRD), financed from the

European Social Fund and by the Romanian Government under the project number POSDRU/159/1.5/S/134378.

## References

1. Vo-Minh, T., Tjahjowidodo, T., Ramon, H., Van Brussel, H. (2011) *A New Approach to Modelling Hysteresis in a Pneumatic Artificial Muscle Using the Maxwell-Slip Model*. IEEE/ASME Transactions on Mechatronics, ISSN 1083-4435, Vol. 16, No. 1 (February 2011), p. 177-186
2. Tondu, B., Lopez, P. (2000) *Modelling and Control of McKibben Muscle Robot Actuators*. IEEE Control Systems Magazine, ISSN 1053-5888/00, Vol. 20, No. 2 (April 2000), p. 15-38
3. Sora, C. (1982) *Bazele electrotehnicii (Electromagnetism)*. Editura Didactică și Pedagogică, București, România (in Romanian), p.487-492
4. Lilly, J.H., Yang, L. (2005) *Sliding Mode Tracking for Pneumatic Muscle Actuators in Opposing Pair Configuration*. IEEE Transactions on Control Systems Technology, ISSN 1063-6536, Vol. 13, No. 4 (July 2005), p. 550-558
5. Doumit, M., Fahim, A., Munro, M. (2009) *Analytical Modelling and Experimental Validation of the Braided Pneumatic Muscle*. IEEE Transactions on Robotics, ISSN 1552-3098, Vol. 25, No. 6 (December 2009), p. 1282-1291
6. Dănilă, A. (2013) *Modelarea și identificarea sistemelor dinamice (Dynamic Systems Modelling and Identification)*. Editura Universității Transilvania din Brașov, ISBN 978-606-19-0271-2, p. 134-138, Brașov, România (in Romanian)
7. Chou, C.-P., Hannaford, B. (1996) *Measurement and Modelling of McKibben Pneumatic Artificial Muscles*. IEEE Transactions on Robotics and Automation, ISSN 1042-296X/96, Vol. 12, No. 1 (February 1996), p. 90-102
8. Babeș, I.M. (2012) *Cercetări privind echipamentele de reabilitare a articulațiilor portante acționate cu ajutorul mușchilor pneumatici (Research concerning pneumatic muscle actuated rehabilitation equipment of bearing joints)*. PhD thesis, Transylvania University of Brasov, Romania, p. 152-166 (in Romanian)
9. Deaconescu, T., Deaconescu, A. (2013) *Functional Characteristics of Pneumatic Muscle Actuated Rehabilitation Equipment for the Joints of the Inferior Limb*. Advanced Science Letters, ISSN 1936-6612, Vol. 19, No. 1, p. 85-89

Received in October 2014